PTEP

Prog. Theor. Exp. Phys. **2016**, 053B01 (18 pages)
DOI: 10.1093/ptep/ptw038

Gauge coupling unification in $SO(32)$ heterotic string theory with magnetic fluxes

Hiroyuki Abe[1], Tatsuo Kobayashi[2,*], Hajime Otsuka[1,*], Yasufumi Takano[2,*], and Takuya H. Tatsuishi[2]

[1]*Department of Physics, Waseda University, Tokyo 169-8555, Japan*
[2]*Department of Physics, Hokkaido University, Sapporo 060-0810, Japan*
[*]E-mail: kobayashi@particle.sci.hokudai.ac.jp, h.otsuka@aoni.waseda.jp, takano@particle.sci.hokudai.ac.jp

Received December 11, 2015; Revised March 6, 2016; Accepted March 7, 2016; Published May 5, 2016

We study $SO(32)$ heterotic string theory on a torus with magnetic fluxes. Non-vanishing fluxes can lead to non-universal gauge kinetic functions for $SU(3) \times SU(2) \times U(1)_Y$, which is an important feature of $SO(32)$ heterotic string theory in contrast to the $E_8 \times E_8$ theory. It is found that the experimental values of gauge couplings are realized with $\mathcal{O}(1)$ values of moduli fields based on realistic models with the $SU(3) \times SU(2) \times U(1)_Y$ gauge symmetry and three chiral generations of quarks and leptons without chiral exotics.

Subject Index B40, B41

1. Introduction

Gauge coupling unification is a familiar tool to search for the underlying theory of the standard model such as the grand unified theory (GUT) or string theory. For example, in the light of the observed values of gauge couplings, the three gauge couplings are unified with the GUT normalization of $U(1)_Y$ at the so-called GUT scale, 2×10^{16} GeV in the low-energy or multi-TeV scale minimal supersymmetric standard model (MSSM). On the other hand, the three gauge couplings are not unified with the GUT normalization of $U(1)_Y$ in the standard model (SM).

Superstring theory also has a certain prediction. In particular, in 4D low-energy effective field theory derived from heterotic string theory, the gauge couplings at tree level are unified up to Kač–Moody levels κ_a at the string scale [1], which is of $\mathcal{O}(10^{17})$ GeV [2]. This prediction is very strong. In order to explain the experimental values, we may need some corrections, e.g. stringy threshold corrections [3–5]. (For numerical studies, see, e.g., Refs. [6–10].) Then, we may need $\mathcal{O}(10)$ moduli values in string units $2\pi\sqrt{\alpha'} = 1$, with α' being the Regge slope.[1] When some moduli values are of $\mathcal{O}(10)$ or larger, the string coupling may become strong and perturbative description may not be valid.

On the other hand, in D-brane models, gauge couplings seem to be independent of each other for gauge sectors, which originate from different sets of D-branes. Thus, one may be able to fit parameters such as moduli values in order to explain the experimental values of three gauge couplings, although some relations and/or constraints may appear [12,13] in a certain type of model.

[1] For a recent study, see [11], where it was pointed out that $\mathcal{O}(1)$ moduli values can be sufficient.

Funded by SCOAP[3]

Here, we study another possible correction within the framework of heterotic string theory. Recently, we carried out systematic analysis towards realistic models within the framework of $SO(32)$ heterotic string theory on the toroidal compactification with magnetic fluxes [14]. In this type of model building, we have constructed models which have the gauge symmetry including $SU(3) \times SU(2) \times U(1)_Y$ and three generations of quarks and leptons as chiral massless spectra. Furthermore, in this paper we show that the gauge couplings depend on magnetic fluxes in this type of $SO(32)$ heterotic string theory. That is, gauge couplings can be non-universal at the string scale and non-universal parts depend on the Kähler moduli, although $E_8 \times E_8$ heterotic string theory with magnetic fluxes cannot lead to non-universal gauge couplings between $SU(3)$ and $SU(2)$ appearing in one E_8.[2] Such non-universal corrections can make the gauge coupling prediction consistent with experimental values. Although such possibilities are proposed in Ref. [17,18], we study numerically the gauge couplings of $SU(3) \times SU(2) \times U(1)_Y$ in more realistic models.

This paper is organized as follows. In Sect. 2, we review 4D low-energy effective field theory derived from $SO(32)$ heterotic string theory with magnetic fluxes. We also review our model building toward realistic models, which have the gauge symmetry including $SU(3) \times SU(2) \times U(1)_Y$ and three chiral generations of quarks and leptons as well as vector-like matter fields in massless spectra. In Sect. 3, we study the gauge couplings and show how non-universal gauge couplings appear in our models. In Sect. 4, we study the gauge couplings numerically in explicit models. Section 5 is devoted to conclusions and discussions.

2. $SO(32)$ heterotic string theory on tori with $U(1)$ magnetic fluxes

In this section, we give a review of the low-energy effective field theory derived from $SO(32)$ heterotic string theory on factorizable tori with $U(1)$ magnetic fluxes. We also show the consistency conditions for $U(1)$ magnetic fluxes which give the constraints for the heterotic string models. (For details of model construction, see, e.g., Ref. [14].)

2.1. *Low-energy effective action of $SO(32)$ heterotic string theory*

First of all, we show the bosonic part of 10D effective supergravity action derived from the $SO(32)$ heterotic string theory on a general complex manifold M with multiple $U(1)$ magnetic fluxes. By calculating the relevant scattering amplitudes on the worldsheet up to order $\mathcal{O}(\alpha')$, we obtain the string-frame bosonic action in the notation of Refs. [17–20],

$$S_{\rm bos} = \frac{1}{2\kappa_{10}^2}\int_{M^{(10)}} e^{-2\phi_{10}}\left[R + 4d\phi_{10}\wedge *d\phi_{10} - \frac{1}{2}H\wedge *H\right] - \frac{1}{2g_{10}^2}\int_{M^{(10)}} e^{-2\phi_{10}}{\rm tr}\,(F\wedge *F), \tag{1}$$

where the gauge and gravitational couplings are set by $g_{10}^2 = 2(2\pi)^7\left(\alpha'\right)^3$ and $2\kappa_{10}^2 = (2\pi)^7\left(\alpha'\right)^4$, respectively. The string coupling is determined by the vacuum expectation value of the ten-dimensional dilaton ϕ_{10}, that is, $g_s = e^{\langle\phi_{10}\rangle}$. The field strength of $SO(32)$ gauge group F has the index of vector representation, which can be normalized as ${\rm tr}_v(T_aT_b) = 2\delta_{ab}$. In addition, the

[2] The low-energy massless spectra were studied within the 10D E_8 theory on a torus with magnetic fluxes from the field-theoretical viewpoint [15,16].

heterotic three-form field strength H is defined by

$$H = dB^{(2)} - \frac{\alpha'}{4}(w_{\rm YM} - w_L), \tag{2}$$

where the part of the α' corrections are characterized by the gauge and gravitational Chern–Simons three-forms, $w_{\rm YM}$ and w_L, respectively.

By the ten-dimensional Hodge duality, the Kalb–Ramond two-form $B^{(2)}$ and its dual six-form $B^{(6)}$ are related as

$$*dB^{(2)} = e^{2\phi_{10}} dB^{(6)}. \tag{3}$$

Then, from the 10D bosonic action (1), we can extract the kinetic term of the Kalb–Ramond field,

$$\begin{aligned} S_{\rm kin} + S_{\rm WZ} = &-\frac{1}{4\kappa_{10}^2}\int_{M^{(10)}} e^{2\phi_{10}} dB^{(6)} \wedge *dB^{(6)} \\ &+ \frac{\alpha'}{8\kappa_{10}^2}\int_{M^{(10)}} B^{(6)} \wedge \left({\rm tr}F^2 - {\rm tr}R^2 - 4(2\pi)^2 \sum_a N_a \delta(\Gamma_a) \right), \end{aligned} \tag{4}$$

where we have added the Wess–Zumino terms induced by the magnetic sources for the Kalb–Ramond field $B^{(6)}$, i.e., stacks of N_a five-branes with their tension being $T_5 = \left((2\pi)^5 (\alpha')^3 \right)^{-1}$. Note that these heterotic five-branes wrap the holomorphic two-cycles Γ_a and their Poincaré dual four-forms are denoted by $\delta(\Gamma_a)$.

When we study $SO(32)$ heterotic string theory on three 2-tori, $M = (T^2)_1 \times (T^2)_2 \times (T^2)_3$, the tadpole cancellation is obtained by solving the equation of motion for the Kalb–Ramond field,

$$\int_{(T^2)_i \times (T^2)_j} \left({\rm tr}\bar{F}^2 - 4(2\pi)^2 \sum_a N_a \delta(\Gamma_a) \right) = 0, \tag{5}$$

where $\bar{F}$ represents the internal $U(1)$ gauge field strengths. These conditions should be satisfied on any four-cycles $(T^2)_i \times (T^2)_j$ with $i \neq j$, $i, j = 1, 2, 3$. Therefore, if the non-vanishing fluxes are not canceled by themselves, five-branes would contribute to the tadpole cancellation [21–23].

2.2. *Axionic coupling through the Green–Schwarz term*

In addition to the effective action (1), the loop effects induce the Green–Schwarz term at the string frame [24,25],

$$S_{\rm GS} = \frac{1}{24(2\pi)^5 \alpha'} \int B^{(2)} \wedge X_8, \tag{6}$$

whose normalization factor is determined by its S-dual type I theory as shown in [26], and the anomaly eight-form X_8 reads

$$X_8 = \frac{1}{24}{\rm Tr}F^4 - \frac{1}{7200}\left({\rm Tr}F^2\right)^2 - \frac{1}{240}\left({\rm Tr}F^2\right)\left({\rm tr}R^2\right) + \frac{1}{8}{\rm tr}R^4 + \frac{1}{32}\left({\rm tr}R^2\right)^2, \tag{7}$$

where "Tr" stands for the trace in the adjoint representations of the $SO(32)$ gauge group.

As pointed out in Refs. [17,18,27], the gauge and gravitational anomalies for the (non-)Abelian gauge groups are canceled by the above Green–Schwarz term (6) and the tadpole condition (5). It is remarkable that when the Abelian gauge symmetries are anomalous, the Abelian gauge bosons become massive due to the Green-Schwarz coupling given by Eq. (6). Therefore, in order to ensure that the hypercharge gauge boson is massless, they should not couple to the axions which are Hodge dual to the Kalb–Ramond fields.

Let us study the couplings between the hypercharge $U(1)_Y$ gauge boson and the axions, explicitly. First of all, we decompose the $SO(32)$ gauge group into the standard-model-like gauge group,

$$SO(32) \to SU(3)_C \otimes SU(2)_L \otimes_{a=1}^{13} U(1)_a, \tag{8}$$

which can be realized by inserting all the multiple $U(1)$ constant magnetic fluxes.

Within the 16 Cartan elements H_i ($i = 1, \ldots, 16$) in the $SO(32)$ gauge group, the Cartan elements of $SU(3)$ are chosen along $H_1 - H_2$ and $H_1 + H_2 - 2H_3$, and that of $SU(2)$ is taken as $H_5 - H_6$, whereas the other Cartan directions of $SO(32)$ are defined in the basis H_i,

$$\begin{aligned}
U(1)_1 &: \ (0,0,0,0,1,1;0,0,\ldots,0),\\
U(1)_2 &: \ (1,1,1,1,0,0;0,0,\ldots,0),\\
U(1)_3 &: \ (1,1,1,-3,0,0;0,0,\ldots,0),\\
U(1)_4 &: \ (0,0,0,0,0,0;1,0,\ldots,0),\\
U(1)_5 &: \ (0,0,0,0,0,0;0,1,\ldots,0),\\
&\vdots\\
U(1)_{13} &: \ (0,0,0,0,0,0;0,0,\ldots,1),
\end{aligned} \tag{9}$$

whose generators, T_a, are normalized so as to satisfy $\mathrm{tr}(T_a T_b) = 2\delta_{ab}$,

$$\begin{aligned}
T_1 &= \frac{1}{\sqrt{2}}\mathrm{diag}\,(0,0,0,0,1,1,0,0,\ldots,0),\\
T_2 &= \frac{1}{2}\mathrm{diag}\,(1,1,1,1,0,0,0,0,\ldots,0),\\
T_3 &= \frac{1}{\sqrt{12}}\mathrm{diag}\,(1,1,1,-3,0,0,0,0,\ldots,0),\\
T_4 &= \mathrm{diag}\,(0,0,0,0,0,0,1,0,\ldots,0),\\
T_5 &= \mathrm{diag}\,(0,0,0,0,0,0,0,1,0,\ldots,0),\\
&\vdots\\
T_{13} &= \mathrm{diag}\,(0,0,0,0,0,0,0,0,\ldots,1).
\end{aligned} \tag{10}$$

Furthermore, when these $U(1)$ fluxes are inserted along the Cartan direction of $SO(32)$, the field strengths of the $U(1)$s are also decomposed into the four- and extra-dimensional parts f, $\bar{f}$, respectively. Then we can dimensionally reduce the one-loop Green–Schwarz term (6) to

$$S_{\mathrm{GS}} = \frac{1}{(2\pi)^3 l_s^2}\int_{M^{(10)}} B^{(2)} \wedge \frac{1}{144}\left(\mathrm{Tr}F\bar{f}^3\right) \tag{11}$$

$$- \frac{1}{(2\pi)^3 l_s^2}\int_{M^{(10)}} B^{(2)} \wedge \frac{1}{2880}\left(\mathrm{Tr}F\bar{f}\right) \wedge \left(\frac{1}{15}\mathrm{Tr}\bar{f}^2 + \mathrm{tr}\bar{R}^2\right) \tag{12}$$

$$+ \frac{1}{(2\pi)^3 l_s^2}\int_{M^{(10)}} B^{(2)} \wedge \left[\frac{1}{96}\left(\mathrm{Tr}F^2\bar{f}^2\right) - \frac{1}{43200}\left(\mathrm{Tr}F\bar{f}\right)^2\right] \tag{13}$$

$$- \frac{1}{(2\pi)^3 l_s^2}\int_{M^{(10)}} B^{(2)} \wedge \frac{1}{5760}\left(\mathrm{Tr}F^2\right) \wedge \left(\frac{1}{15}\mathrm{Tr}\bar{f}^2 + \mathrm{tr}\bar{R}^2\right) \tag{14}$$

$$+ \frac{1}{(2\pi)^3 l_s^2}\int_{M^{(10)}} B^{(2)} \wedge \frac{1}{384}\left(\mathrm{tr}R^2\right) \wedge \left(\mathrm{tr}\bar{R}^2 - \frac{1}{15}\mathrm{Tr}\bar{f}^2\right), \tag{15}$$

where $l_s = 2\pi\sqrt{\alpha'}$ and F denote the field strengths of $SU(3)_C$, $SU(2)_L$, and $U(1)_a$, $(a = 1, \ldots, 13)$.

From here, we write the Kalb–Ramond field $B^{(2)}$ and internal $U(1)_a$ field strengths $\bar{f}_a$, $(a = 1, \ldots, 13)$ in the basis of Kähler forms w_i on tori $\left(T^2\right)_i$,

$$B^{(2)} = b_S^{(2)} + l_s^2 \sum_{i=1}^{3} b_i^{(0)} w_i,$$
$$\bar{f}_a = 2\pi \sum_{i=1}^{3} m_a^i w_i, \tag{16}$$

where m_a^i are the $U(1)_a$ fluxes constrained by the Dirac quantization condition. From Eqs. (11) and (12), we can extract the Stueckelberg couplings between the $U(1)$ gauge fields and the universal axion $b_S^{(0)}$, which is the Hodge dual of the tensor field $b_S^{(2)}$,

$$\frac{1}{3\,(2\pi)^3\, l_s^2} \int b_S^{(2)} \wedge \Bigg[\mathrm{tr} T_1^4 \bar{f}_1^3 f_1 + \left(\mathrm{tr} T_2^4 \bar{f}_2^3 + 3\left(\mathrm{tr} T_2^2 T_3^2\right) \bar{f}_2 \bar{f}_3^2 + \left(\mathrm{tr} T_2 T_3^3\right) \bar{f}_3^3\right) f_2$$
$$+ \left(\mathrm{tr} T_3^4 \bar{f}_3^3 + 3\left(\mathrm{tr} T_2 T_3^3\right) \bar{f}_2 \bar{f}_3^2 + 3\left(\mathrm{tr} T_2^2 T_3^2\right) \bar{f}_2^2 \bar{f}_3\right) f_3 + \sum_{c=4}^{13} \mathrm{tr} T_c^4 \bar{f}_c^3 f_c \Bigg], \tag{17}$$

which implies that one of the multiple $U(1)$ gauge fields absorbs the universal axion and becomes massive. As shown in Sect. 3, the hypercharge $U(1)_Y$ is identified with the linear combinations of multiple $U(1)$s, i.e., $U(1)_Y = \frac{1}{6}(U(1)_3 + 3\sum_c U(1)_c)$, where the summation over c depends on the concrete models. In such cases, the $U(1)_Y$ gauge field becomes massless under

$$6\mathrm{tr}\left(T_3^4\right) m_3^1 m_3^2 m_3^3 + 3\mathrm{tr}\left(T_2 T_3^3\right) \sum_{i,j,k=1}^{3} d_{ijk} m_2^i m_3^j m_3^k + 3\mathrm{tr}\left(T_2^2 T_3^2\right) \sum_{i,j,k=1}^{3} d_{ijk} m_2^i m_2^j m_3^k$$
$$+ 18 \sum_{c=4}^{13} \mathrm{tr}\left(T_c^4\right) m_c^1 m_c^2 m_c^3 = 0, \tag{18}$$

where d_{ijk} denotes the intersection number and the non-vanishing intersection numbers of 2-tori appear, $d_{ijk} = 1\ (i \neq j \neq k)$.

In addition to the universal axion, other axions also appear from the associated internal two-cycles, which are known as the Kähler axions. When the dual field $B^{(6)}$ is expanded as

$$B^{(6)} = l_s^6 b_S^{(0)} \mathrm{vol}\,(M) + l_s^4 \sum_{k=1}^{3} b_k^{(2)} \hat{w}_k, \tag{19}$$

where $\mathrm{vol}(M)$ is the volume-form on the six-dimensional space M and $\hat{w}_k$ are the Hodge dual four-forms of the Kähler forms, we can extract the axionic couplings between Kähler axions and the $U(1)$ gauge bosons through Eq. (4),

$$\frac{1}{l_s^2} \int b_i^{(2)} \wedge \sum_{a=1}^{13} \mathrm{tr}\,(T_a T_a)\, f_a m_a^i, \tag{20}$$

which leads to the following $U(1)_Y$ massless condition,

$$\mathrm{tr}\,(T_3T_3)\,m_3^i + 3\sum_{c=4}^{13}\mathrm{tr}\big(T_cT_c\big)m_c^i = 0, \tag{21}$$

with $i = 1, 2, 3$.

2.3. *Model building and constraints*

Here we review our approach to constructing realistic models (for full details, see Ref. [14]). So far, we have introduced the magnetic fluxes m_a^i along all $U(1)_a$ for $a = 1, \ldots, 13$. In our model, such magnetic fluxes break $SO(32)$ into $SU(3)_C \times SU(2)_L \times \prod_{a=1}^{13} U(1)_a$ and a certain linear combination of $\prod_{a=1}^{13} U(1)_a$ corresponds to $U(1)_Y$. However, the degenerate magnetic fluxes lead to the enhancement of gauge symmetry, e.g., $SU(4) \times SU(2) \times SU(2)$ in the visible sector. In such a case, we introduce Wilson lines to break this remaining large gauge group into $SU(3)_C \times SU(2)_L \times U(1)_Y$.

In addition to gauge symmetry breaking, non-vanishing magnetic fluxes can realize the 4D chiral theory, where the number of zero modes is determined by their $U(1)$ charges and magnetic fluxes. The relevant matter contents in the SM reside in the adjoint and vector representations of $SO(12)$ in $SO(32)$ and their generation numbers are given by

$$\begin{aligned}
m_{Q_1} &= \prod_{i=1}^{3} m^i_{Q_1} = \prod_{i=1}^{3}\left(m_1^i + m_2^i + m_3^i\right), & m_{Q_2} &= \prod_{i=1}^{3} m^i_{Q_2} = \prod_{i=1}^{3}(-m_1^i + m_2^i + m_3^i),\\
m_{L_1} &= \prod_{i=1}^{3} m^i_{L_1} = \prod_{i=1}^{3}\left(m_1^i + m_2^i - 3m_3^i\right), & m_{L_2} &= \prod_{i=1}^{3} m^i_{L_2} = \prod_{i=1}^{3}(-m_1^i + m_2^i - 3m_3^i),\\
m_{u^c_{R_1}} &= \prod_{i=1}^{3} m^i_{u^c_{R_1}} = \prod_{i=1}^{3}(-4m_3^i), & m_{n_1} &= \prod_{i=1}^{3} m^i_{n_1} = \prod_{i=1}^{3}(2m_1^i),\\
m_{d^c_{R_1}} &= \prod_{i=1}^{3} m^i_{d^c_{R_1}} = \prod_{i=1}^{3}(2m_2^i + 2m_3^i), & m_{d^c_{R_2}} &= \prod_{i=1}^{3} m^i_{d^c_{R_2}} = \prod_{i=1}^{3}(-2m_2^i + 2m_3^i),\\
m_{L_3^a} &= \prod_{i=1}^{3} m^i_{L_3^a} = \prod_{i=1}^{3}(m_1^i - m_a^i), & m_{L_4^a} &= \prod_{i=1}^{3} m^i_{L_4^a} = \prod_{i=1}^{3}(-m_1^i - m_a^i),\\
m_{u^{ca}_{R_2}} &= \prod_{i=1}^{3} m^i_{u^{ca}_{R_2}} = \prod_{i=1}^{3}(-m_2^i - m_3^i - m_a^i), & m_{d^{ca}_{R_3}} &= \prod_{i=1}^{3} m^i_{d^{ca}_{R_3}} = \prod_{i=1}^{3}(-m_2^i - m_3^i + m_a^i),\\
m_{e^{ca}_{R_1}} &= \prod_{i=1}^{3} m^i_{e^{ca}_{R_1}} = \prod_{i=1}^{3}(-m_2^i + 3m_3^i + m_a^i), & m_{n_2^a} &= \prod_{i=1}^{3} m^i_{n_2^a} = \prod_{i=1}^{3}(-m_2^i + 3m_3^i - m_a^i),
\end{aligned} \tag{22}$$

where $Q_{1,2}$ are the left-handed quarks, $L_{1,2}$, $L^a_{3,4}$ are the charged leptons and/or Higgs, $u^c_{R_1}$, $u^{ca}_{R_2}$ are the charge conjugate of right-handed up-type quarks, $d^c_{R_{1,2}}$, $d^{ca}_{R_3}$ are the charge conjugate of right-handed down-type quarks, $e^{ca}_{R_1}$ are the charge conjugate of right-handed leptons, and n_1, n_2^a are the singlets in the standard model gauge groups.

It is remarkable that there are constraints for these $U(1)$ magnetic fluxes. First, there are the $U(1)_Y$ massless conditions (18) and (21) by taking account of the axionic couplings with $U(1)_Y$ gauge

boson. Furthermore, there are the tadpole conditions given by Eq. (5). When the heterotic five-branes are absent in our system, Eq. (5) is rewritten as

$$\sum_{a=1}^{13} \mathrm{tr}\left(T_a T_a\right) m_a^i m_a^j = 0, \quad i \neq j, \quad (i, j = 1, 2, 3)\,, \tag{23}$$

which are required from the consistencies of heterotic string theory.

Without the existence of the heterotic five-branes, it is known that $U(1)$ magnetic fluxes satisfy the so-called K-theory constraints, e.g., Ref. [17,18],

$$\sum_{a=1}^{13} m_a^i = 0 \pmod 2, \tag{24}$$

for $i = 1, 2, 3$. These K-theory constraints are discussed in the S-dual to the $SO(32)$ heterotic string theory, that is, type I string theory. (See, for instance, Refs. [28,29].)

Finally, non-vanishing magnetic fluxes generically induce the non-vanishing Fayet–Iliopoulos (FI) terms for $U(1)_a$ with $a = 1, 2, \ldots, 13$. Even if such FI terms are not canceled by themselves, they may be able to be canceled by the vacuum expectation values (VEVs) of scalar fields in the hidden sector.

3. Gauge couplings in heterotic string

In this section, we show the formula of gauge kinetic functions in our model. After dimensionally reducing the 10D effective action (1) as well as the one-loop GS term (6), it is found that the gauge kinetic functions of $SU(3)_C$ and $SU(2)_L$ receive different one-loop threshold corrections depending on the Abelian fluxes, while those of $U(1)_Y$ do not receive such corrections due to the vanishing axionic couplings with the $U(1)_Y$ gauge boson.

3.1. *Gauge couplings at tree level*

After compactifying on a 6D internal manifold M with volume $\mathrm{Vol}(M)$, the 4D reduced Planck scale M_{Pl} and the gauge coupling constant g_4 can be extracted as

$$\begin{aligned} M_{\mathrm{Pl}}^2 &= \frac{g_s^{-2}\mathrm{Vol}\,(M)}{2\kappa_{10}^2}, \\ 2g_4^{-2} &= g_s^{-2}\mathrm{Vol}\,(M)\, g_{10}^{-2}, \end{aligned} \tag{25}$$

which lead to the following relation between the string scale $M_s = 1/l_s$ with $l_s = 2\pi\sqrt{\alpha'}$ being the typical string length, and the Planck scale,

$$M_s^2 = \frac{M_{\mathrm{Pl}}^2}{4\pi\alpha_4^{-1}}, \tag{26}$$

where $\alpha_4^{-1} = 4\pi g_4^{-2}$. Since the four-dimensional gauge coupling is determined by the VEV of the dilaton at the tree level, $\langle \mathrm{Re}\, \mathcal{S}\rangle = g_4^{-2}$, where

$$\mathcal{S} = \frac{1}{\pi}\left(\frac{e^{-2\phi_{10}}\mathrm{Vol}\,(M)}{l_s^6} + i b_S^{(0)}\right), \tag{27}$$

with $b_S^{(0)}$ being the universal axion, the string scale is roughly estimated as

$$M_s \simeq 1.4 \times 10^{17}\,\mathrm{GeV} \tag{28}$$

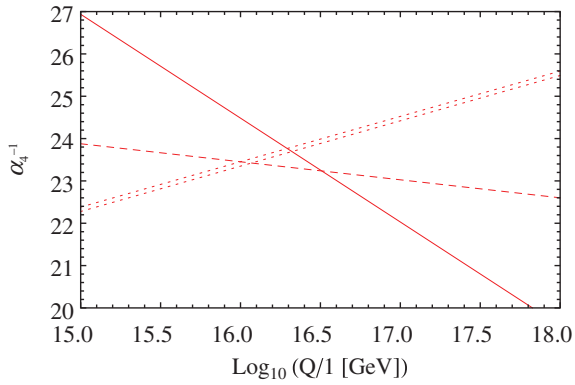

Fig. 1. RG flow of the gauge couplings in the MSSM with GUT normalization at the two-loop level. These lines show the gauge coupling of $U(1)_Y$ (thick line), $SU(2)_L$ (dashed line), and $SU(3)_C$ (dotted line), respectively. Here, we include the error bar associated with the QCD coupling $\alpha^{-1}_{SU(3)_C}$ [30].

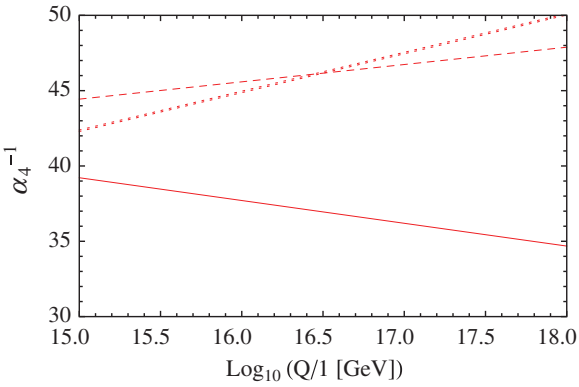

Fig. 2. RG flow of the gauge couplings in the SM with GUT normalization at the two-loop level. These lines show the gauge coupling of $U(1)_Y$ (thick line), $SU(2)_L$ (dashed line), and $SU(3)_C$ (dotted line), respectively.

from Eq. (26) by employing $M_{\rm Pl} = 2.435 \times 10^{18}$ GeV and the four-dimensional gauge coupling constant, $\alpha_4^{-1} \simeq 25$, implied by the renormalization group (RG) equations of the MSSM. As mentioned in Sect. 1, the gauge couplings of SM gauge groups are different from each other at the string scale, as illustrated in Fig. 1 under the assumption that the supersymmetry (SUSY) is broken at the TeV scale and the $U(1)_Y$ gauge coupling is normalized as satisfying the so-called GUT relation. In Fig. 1, we involve two-loop effects to the RG equations. On the other hand, when the SUSY is broken at the string scale, the behavior of gauge couplings from the electroweak scale to the string scale obeys the renormalization group equations of the standard model. As seen in Fig. 2, the gaps between the gauge couplings of non-Abelian gauge groups are better than for MSSM. However, it requires slight corrections to coincide with the unified one at the string scale. In this case, the string scale is estimated as $M_s \simeq 1.0 \times 10^{17}$ GeV by use of $\alpha_4^{-1} \simeq 45$. We also employ experimental values such as the gauge coupling of $SU(3)$, $\alpha^{-1}_{SU(3)_C} \simeq 0.1184$, the Weinberg angle $\sin^2\theta \simeq 0.231$, and the fine-structure constant $\alpha \simeq 1/128$ at the electroweak scale [30] in Figs. 1 and 2.

3.2. The one-loop threshold corrections

As shown in the previous section, the dilaton $\mathcal{S}$ gives the universal gauge kinetic function. However, the Green–Schwarz term (6), in particular (13) and (14), can lead to non-universal gauge kinetic

functions [17,18]. Indeed, we obtain the non-universal axionic couplings

$$S_{\rm GS} \supset \frac{1}{(2\pi)^3}\sum_{k=1}^{3}\int_{M^{1,3}} b_k^{(0)}{\rm tr}_{SU(3)}F^2\int_{T^2\times T^2\times T^2} w_k\wedge\left(\frac{1}{8}{\rm tr}\left(T_2^2\right)\bar{f}_2^2\right)$$
$$+\frac{1}{(2\pi)^3}\sum_{k=1}^{3}\int_{M^{1,3}} b_k^{(0)}{\rm tr}_{SU(2)}F^2\int_{T^2\times T^2\times T^2} w_k\wedge\left(\frac{1}{4}{\rm tr}\left(T_1^2\right)\bar{f}_1^2\right), \tag{29}$$

which lead to the non-universal gauge kinetic functions. This is because we insert the different $U(1)$ fluxes between the $U(1)_1$ and $U(1)_2$ Cartan directions. Such structures are typical in $SO(32)$ heterotic string theory which is expected as the S-dual of type I string theory with several D-branes. However, the non-universal gauge kinetic functions for $SU(3)_C$ and $SU(2)_L$ cannot be seen in $E_8\times E_8$ heterotic string theory due to the trace identities, ${\rm Tr}\left(F^4\right)=\frac{1}{100}\left({\rm Tr}\left(F^2\right)\right)^2$, where F denotes the gauge field strength of E_8. From these trace identities, Eq. (13) is regarded as the type of Eq. (14). Therefore, the gauge kinetic functions of $SU(3)_C$ and $SU(2)_L$ are equal to each other. It might be preferred in the non-supersymmetric theory such as the standard model from Fig. 2, although some other threshold corrections are required to unify the gauge couplings.

When we define the Kähler moduli as

$$\mathcal{T}_k = t_k + ib_k^{(0)}, \tag{30}$$

where t_k corresponds to the volume of $\left(T^2\right)_k$ in string units,[3] the gauge kinetic functions of $SU(3)_C$ and $SU(2)_L$ become

$$f_{SU(3)_C} = \mathcal{S}+\sum_{k=1}^{3}\beta_3^k\mathcal{T}_k,$$
$$f_{SU(2)_L} = \mathcal{S}+\sum_{k=1}^{3}\beta_2^k\mathcal{T}_k, \tag{31}$$

where

$$\beta_3^k=\frac{\left(d_2\right)^2}{8\pi}\sum_{i,j=1}^{3}d_{ijk}m_2^im_2^j,\quad \beta_2^k=\frac{\left(d_1\right)^2}{4\pi}\sum_{i,j=1}^{3}d_{ijk}m_1^im_1^j, \tag{32}$$

with $d_1=\sqrt{2}$ and $d_2=2$. Note that the threshold corrections depend on the magnetic fluxes.

On the other hand, $U(1)_Y$ is defined as linear combinations of multiple $U(1)$s so as to derive the matter contents in the standard model (for details, see Ref. [14]),

$$U(1)_Y=\frac{1}{6}\left(U(1)_3+3\sum_{c=4}^{N}U(1)_c\right), \tag{33}$$

where the normalization of $U(1)_Y$ is then determined by

$$\frac{1}{\alpha_{U(1)_Y}}=\frac{{\rm tr}\left(T_3T_3\right)}{36\,\alpha_{U(1)_3}}+\sum_{c=4}^{N}\frac{{\rm tr}\left(T_cT_c\right)}{4\,\alpha_{U(1)_c}}=\left(\frac{1}{3}+\frac{N-3}{4}\right)4\pi\,{\rm Re}\,\langle\mathcal{S}\rangle, \tag{34}$$

in which ${\rm tr}(T_3T_3)=12$, ${\rm tr}(T_cT_c)=1$. Since the threshold corrections do not appear due to the vanishing axionic couplings with the $U(1)_Y$ gauge boson, the gauge kinetic function of $U(1)_Y$ is

[3] Here and in what follows, we work in string units, $2\pi\sqrt{\alpha'}=1$, unless otherwise specified.

extracted as

$$f_{U(1)_Y} = \left(\frac{1}{3} + \frac{N-3}{4}\right)\mathcal{S}. \tag{35}$$

4. Numerical studies in explicit models

In this section, we show the models satisfying the consistency conditions in Sect. 2.3, where the chiral massless spectra in the visible sector are just three generations of quarks and leptons without chiral exotics, and at the same time the experimental values of gauge couplings are realized at the string scale. Although there are extra vector-like visible matter fields and hidden chiral and vector-like matter fields, we assume that these modes become massive around M_s.

4.1. Standard-model scenario

The non-vanishing $U(1)_a$ magnetic fluxes generate the D_a terms for $U(1)_a$, that is, the FI terms,

$$D_a = \sum_{i=1}^{3} \frac{m_a^i}{\mathcal{A}_i}, \tag{36}$$

where $\mathcal{A}_i = (2\pi R_i)^2 \mathrm{Im}\,\tau_i$ and τ_i are the areas and complex structure moduli of the tori $\left(T^2\right)_i$. Since, in general, these FI terms are non-vanishing, they induce mass splitting between the SM particles and their superpartners due to the SUSY-breaking of the order of the string scale, M_s.

Although, in our model, an unbroken gauge sector retains the $\mathcal{N} = 4$ SUSY at the tree level, the non-vanishing FI terms also give rise to the mass terms for them except for the gauge bosons at the loop level. The typical mass scale is of

$$\mathcal{O}\left(\frac{g_a^2}{(4\pi)^2} M_s\right), \tag{37}$$

where g_a is the gauge coupling of the extra $U(1)_a$ [31]. From now on, below the string scale M_s, we consider the scenario where the matter contents in the visible sector are just those of the SM and we study the gauge couplings of the SM numerically.[4]

First of all, the $U(1)_Y$ gauge coupling $g^2_{U(1)_Y}$ at M_s is determined only by $\langle\mathcal{S}\rangle$ and N through Eq. (35),

$$\frac{1}{g^2_{U(1)_Y}(M_s)} = A(N)\,\langle\mathcal{S}\rangle, \tag{38}$$

where

$$A(N) = \left(\frac{1}{3} + \frac{N-3}{4}\right). \tag{39}$$

From the experimental values of $U(1)_Y$ gauge coupling, $g^{-2}_{U(1)_Y}(M_s) = 4.80$ for the SM, the dilaton VEV $\langle\mathcal{S}\rangle$ is determined by N as shown in Table 1 for $N = 5, 7, 9$. In what follows, we discuss the explicit models with $N = 5, 7, 9$.

[4] We can ignore the threshold corrections appearing from the adjoint matter because they are small enough, as pointed out in Ref. [13].

Table 1. The VEV of dilaton $\langle \mathcal{S} \rangle$ for the SM.

N	5	7	9
$\langle \mathcal{S} \rangle$	5.76	3.60	2.62

Table 2. The values of B_2 and B_3 for the SM in the case of $N = 5, 7, 9$. By increasing the number of N appearing in the definition of $U(1)_Y$ (33), the values of B_i increase.

	Model 1 ($N = 5$)	Model 2 ($N = 7$)	Model 3 ($N = 9$)
B_2	-6.42	0.36	3.45
B_3	-6.24	0.55	3.63

Next, by solving Eq. (31) and the two-loop renormalization group equations for the SM, we evaluate the ratio of gauge couplings at M_s as

$$\frac{\left\langle \mathrm{Re}\, f_{U(1)_Y} \right\rangle}{\left\langle \mathrm{Re}\, f_3 \right\rangle} = \frac{A(N)}{1 + \sum_k \beta_3^k \langle \mathcal{T}_k \rangle / \langle \mathcal{S} \rangle} = \frac{g_3^2(M_s)}{g_{U(1)_Y}^2(M_s)} \simeq 1.272,$$
$$\frac{\left\langle \mathrm{Re}\, f_{U(1)_Y} \right\rangle}{\left\langle \mathrm{Re}\, f_2 \right\rangle} = \frac{A(N)}{1 + \sum_k \beta_2^k \langle \mathcal{T}_k \rangle / \langle \mathcal{S} \rangle} = \frac{g_2^2(M_s)}{g_{U(1)_Y}^2(M_s)} \simeq 1.292 \tag{40}$$

for the SM. Here, the experimental values such as the gauge coupling of $SU(3)$, $\alpha_{SU(3)_C}^{-1} \simeq 0.1184$, the Weinberg angle $\sin^2\theta \simeq 0.231$, and the fine-structure constant $\alpha \simeq 1/128$ at the electroweak scale are employed. From Eq. (40), we estimate the following quantities in Table 2 for $N = 5, 7, 9$,

$$B_2 = \pi \sum_{k=1}^{3} \beta_2^k \langle \mathcal{T}_k \rangle = m_1^2 m_1^3 \langle \mathcal{T}_1 \rangle + m_1^3 m_1^1 \langle \mathcal{T}_2 \rangle + m_1^1 m_1^2 \langle \mathcal{T}_3 \rangle,$$
$$B_3 = \pi \sum_{k=1}^{3} \beta_3^k \langle \mathcal{T}_k \rangle = m_2^2 m_2^3 \langle \mathcal{T}_1 \rangle + m_2^3 m_2^1 \langle \mathcal{T}_2 \rangle + m_2^1 m_2^2 \langle \mathcal{T}_3 \rangle. \tag{41}$$

When we construct an explicit model, all $U(1)$ magnetic fluxes as well as N appearing in the definition of $U(1)_Y$ given by Eq. (33) are fixed and the β_2^k and β_3^k in Eq. (41) are also fixed hereafter. Then, we can examine whether the $\mathcal{O}(1)$ values of $\langle \mathcal{T}_k \rangle$ are consistent with the values of B_2 and B_3 in Table 2 or not. Although it is expected that one of the unfixed Kähler moduli will appear by solving the two equations (40) under the three Kähler moduli $\langle \mathcal{T}_k \rangle$, in some models there are no solutions for realistic values of $\mathcal{T}_k$, i.e., $\mathcal{T}_k < 0$, $\mathcal{T}_k \ll 1$, $\mathcal{T}_k \gg 1$.

In the following, we show the three examples of magnetic flux configurations denoted by models $1(N = 5)$, $2(N = 7)$, and $3(N = 9)$ which are realistic in the sense that they include the gauge symmetry including $SU(3)_C \times SU(2)_L \times U(1)_Y$, three chiral generations of quarks and leptons without chiral exotics in the visible sector, and the experimental values of gauge couplings in Eq. (40); at the same time, they satisfy the consistency conditions in Sect. 2.3. The procedure of searching for these models is as follows. First, in the light of $U(1)_Y$ massless conditions (18) and (21), we restrict ourselves to the magnetic flux configurations

$$m_3^i = 0,$$
$$m_{3+a}^i = -m_{8+a}^i \ (a = 1, 2, 3, 4, 5), \tag{42}$$

otherwise it is hard to realize the $U(1)_Y$ massless conditions and three generations of quarks and leptons (22) simultaneously. Next, we classify the $U(1)_{1,2}$ magnetic fluxes $m^i_{1,2}$ so that the three generations of left-handed quarks $Q_{1,2}$ and single-valued wavefunction for the singlet n_1 are achieved,

$$\begin{aligned} m_{Q_1} + m_{Q_2} &= \prod_{i=1}^{3}\left(m^i_1 + m^i_2\right) + \prod_{i=1}^{3}\left(-m^i_1 + m^i_2\right) = 3, \\ m^i_{n_1} &= 2m^i_1, \end{aligned} \tag{43}$$

which constrain the $m^i_{1,2}$ to be integers or half-integers. Furthermore, from the K-theory condition (24) with the magnetic flux background (42), the generation of left-handed quarks is determined by $m_{Q_1} = 0$ and $m_{Q_2} = 3$, corresponding to the model "Type B′" in Ref. [14], due to the even numbers of $m^i_1 + m^i_2$ for $i = 1, 2, 3$. Then, the magnetic fluxes $m^i_{1,2}$ should become half-integers.

Thus, from the list obtained for $m^i_{1,2}$, we search for the $\mathcal{O}(1)$ values of Kähler moduli $\langle \mathcal{T}_i \rangle$, $i = 1, 2, 3$ by solving Eq. (41). When $m^3_1 m^2_2 - m^2_1 m^3_2 \neq 0$, the Kähler moduli $\mathcal{T}_{2,3}$ are represented by

$$\begin{aligned} \mathcal{T}_2 &= a_2 \mathcal{T}_1 + b_2, \\ \mathcal{T}_3 &= a_3 \mathcal{T}_1 + b_3, \end{aligned} \tag{44}$$

where $a_{2,3}$ and $b_{2,3}$ are the flux-dependent constants given through Eq. (41), i.e.

$$\begin{aligned} a_2 &= \frac{m^2_1 m^2_2\left(m^1_1 m^3_2 - m^3_1 m^1_2\right)}{m^1_1 m^1_2\left(m^3_1 m^2_2 - m^2_1 m^3_2\right)}, \qquad b_2 = \frac{m^1_2 m^2_2 B_2 - m^1_1 m^2_1 B_3}{m^1_1 m^1_2\left(m^3_1 m^2_2 - m^2_1 m^3_2\right)}, \\ a_3 &= \frac{m^3_1 m^3_2\left(m^1_1 m^2_2 - m^2_1 m^1_2\right)}{m^1_1 m^1_2\left(m^2_1 m^3_2 - m^3_1 m^2_2\right)}, \qquad b_3 = \frac{m^1_2 m^3_2 B_2 - m^1_1 m^3_1 B_3}{m^1_1 m^1_2\left(m^2_1 m^3_2 - m^3_1 m^2_2\right)}. \end{aligned} \tag{45}$$

First of all, we constrain the $U(1)_{1,2}$ magnetic fluxes to realize the $\mathcal{O}(1)$ values of the Kähler moduli. We then determine the other $U(1)_a$ $a = 4, 5, \ldots, 13$ fluxes so as to achieve the matter contents in the standard model in Eq. (22), $U(1)_Y$ massless conditions (18) and (21), and the K-theory condition (24). In a similar way to the case without five-branes, we explore the $U(1)_a$ $a = 1, 2, \ldots, 13$ fluxes under the assumption (42) so as to achieve the experimental values of gauge couplings at the string scale with $\mathcal{O}(1)$ values of Kähler moduli, the matter contents in the standard model in Eq. (22), $U(1)_Y$ massless conditions (18) and (21), and the K-theory condition (24).

As a result, within the range $2m^i_1 \in [-15, 15]$, $1.0 \leq \langle \mathcal{T}_i \rangle \leq 3.5$, $i = 1, 2, 3$, and $1 \leq \mathrm{Vol}(M) \leq 10$, the typical magnetic flux configurations in models 1, 2, 3 with and without heterotic five-branes are determined as shown in Tables 3, 4, and 5, respectively. These flux configurations in all the models induce the non-vanishing FI terms whose size is of $\mathcal{O}(M_s)$. In the case without five-branes in Tables 3, 4, and 5, Eq. (5) is satisfied by the $U(1)$ fluxes themselves, whereas, in the case with five-branes, the tadpole condition (5) is canceled by the existence of the five-branes. Moreover, the magnetic fluxes in Tables 3, 4, and 5 predict the same values of gauge couplings at the string scale, because only m^i_1 and m^i_2 appear in the non-universal terms of $SU(2)_L$ and $SU(3)_C$ gauge couplings.

Finally, Figs. 3, 4, and 5 show the value of the Kähler moduli and the volume of the three-tori $\mathrm{Vol}(M) = \langle \mathcal{T}_1 \mathcal{T}_2 \mathcal{T}_3 \rangle$ as a function of $\langle \mathcal{T}_1 \rangle$ in models 1, 2, and 3, respectively. Note that the axions $b^{(0)}_k$ do not appear in the volume of the three-tori, due to the shift symmetries associated with the

Table 3. The magnetic flux configurations in model 1 with and without five-branes.

Magnetic fluxes	Without five-branes	With five-branes
$\left(2m_1^1, 2m_1^2, 2m_1^3\right)$	$(9, -1, -1)$	$(9, -1, -1)$
$\left(2m_2^1, 2m_2^2, 2m_2^3\right)$	$(3, 1, -3)$	$(3, 1, -3)$
$\left(2m_3^1, 2m_3^2, 2m_3^3\right)$	$(0, 0, 0)$	$(0, 0, 0)$
$\left(2m_4^1, 2m_4^2, 2m_4^3\right)$	$(3, -3, 5)$	$(3, -3, 5)$
$\left(2m_5^1, 2m_5^2, 2m_5^3\right)$	$(3, 3, 3)$	$(3, 3, 3)$
$\left(2m_6^1, 2m_6^2, 2m_6^3\right)$	$(3, 3, 3)$	$(3, 3, 3)$
$\left(2m_7^1, 2m_7^2, 2m_7^3\right)$	$(3, -1, -1)$	$(3, 3, 3)$
$(2m_8^1, 2m_8^2, 2m_8^3)$	$(3, -1, -1)$	$(3, 3, 3)$

Table 4. The magnetic flux configurations in model 2 with and without five-branes.

Magnetic fluxes	Without five-branes	With five-branes
$\left(2m_1^1, 2m_1^2, 2m_1^3\right)$	$(-1, 5, 1)$	$(-1, 5, 1)$
$\left(2m_2^1, 2m_2^2, 2m_2^3\right)$	$(5, 3, -1)$	$(5, 3, -1)$
$\left(2m_3^1, 2m_3^2, 2m_3^3\right)$	$(0, 0, 0)$	$(0, 0, 0)$
$\left(2m_4^1, 2m_4^2, 2m_4^3\right)$	$(-1, -1, -1)$	$(-1, -1, -1)$
$\left(2m_5^1, 2m_5^2, 2m_5^3\right)$	$(-3, -1, -1)$	$(-3, -1, -1)$
$\left(2m_6^1, 2m_6^2, 2m_6^3\right)$	$(3, -3, -1)$	$(3, -3, -1)$
$\left(2m_7^1, 2m_7^2, 2m_7^3\right)$	$(5, -11, 1)$	$(3, -3, -1)$
$\left(2m_8^1, 2m_8^2, 2m_8^3\right)$	$(5, 7, 1)$	$(3, -3, -1)$

Table 5. The magnetic flux configurations in model 3 with and without five-branes.

Magnetic fluxes	Without five-branes	With five-branes
$\left(2m_1^1, 2m_1^2, 2m_1^3\right)$	$(-3, 1, -3)$	$(-3, 1, -3)$
$\left(2m_2^1, 2m_2^2, 2m_2^3\right)$	$(3, 3, -1)$	$(3, 3, -1)$
$\left(2m_3^1, 2m_3^2, 2m_3^3\right)$	$(0, 0, 0)$	$(0, 0, 0)$
$\left(2m_4^1, 2m_4^2, 2m_4^3\right)$	$(-1, -1, -1)$	$(-1, -1, -1)$
$\left(2m_5^1, 2m_5^2, 2m_5^3\right)$	$(-1, -1, -1)$	$(-1, -1, -1)$
$\left(2m_6^1, 2m_6^2, 2m_6^3\right)$	$(-1, -1, -1)$	$(-1, -1, -1)$
$\left(2m_7^1, 2m_7^2, 2m_7^3\right)$	$(3, -3, -1)$	$(3, -3, -3)$
$\left(2m_8^1, 2m_8^2, 2m_8^3\right)$	$(3, -3, -1)$	$(3, -3, -3)$

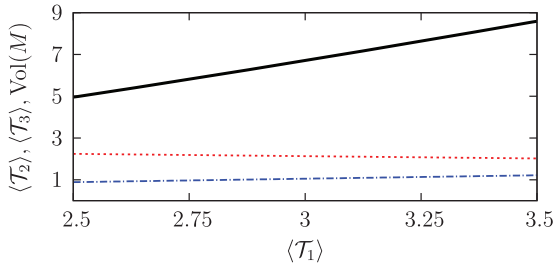

Fig. 3. The VEVs of moduli $\langle \mathcal{T}_2 \rangle$ (red dashed curve), $\langle \mathcal{T}_3 \rangle$ (blue dot-dashed curve), and the volume of three-tori $\mathrm{Vol}(M) = \langle \mathcal{T}_1 \mathcal{T}_2 \mathcal{T}_3 \rangle$ (black thick curve) as a function of $\langle \mathcal{T}_1 \rangle$ in model 1.

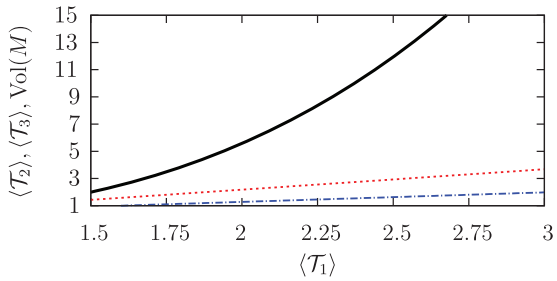

Fig. 4. The VEVs of moduli $\langle \mathcal{T}_2 \rangle$ (red dashed curve), $\langle \mathcal{T}_3 \rangle$ (blue dot-dashed curve), and the volume of three-tori $\mathrm{Vol}(M) = \langle \mathcal{T}_1 \mathcal{T}_2 \mathcal{T}_3 \rangle$ (black thick curve) as a function of $\langle \mathcal{T}_1 \rangle$ in model 2.

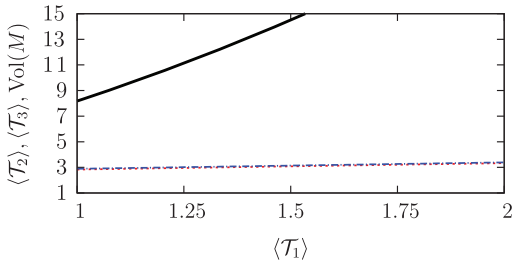

Fig. 5. The VEVs of moduli $\langle \mathcal{T}_2 \rangle$ (red dashed curve), $\langle \mathcal{T}_3 \rangle$ (blue dot-dashed curve), and the volume of three-tori $\mathrm{Vol}(M) = \langle \mathcal{T}_1 \mathcal{T}_2 \mathcal{T}_3 \rangle$ (black thick curve) as a function of $\langle \mathcal{T}_1 \rangle$ in model 3.

Kalb–Ramond field $B^{(2)}$ in Eq. (16). The $\mathcal{O}(1)$ values of the Kähler moduli in Figs. 3, 4, and 5 are consistent with the experimental values of gauge couplings in the SM. Similarly, we can analyze a wider region of $\mathcal{T}_{\min} < \langle \mathcal{T}_i \rangle < \mathcal{T}_{\max}$ with larger $\mathcal{T}_{\max}$ and smaller $T_{\min}$.

4.2. MSSM scenario

As shown in Eq. (36) in Sect. 4.1, in general, the FI terms are non-vanishing. However, the non-vanishing D-terms for extra $U(1)$s generated by the generic magnetic flux background would be canceled by VEVs of hidden scalar fields, and $\mathcal{N} = 1$ SUSY remains when we take the low-energy SUSY breaking scenario. Since the size of the SUSY breaking scale depends on the moduli stabilization scenario, we leave the details for future work. In this respect, we consider the scenario where the SUSY remains at M_s and breaks around 1 TeV, and below M_s the massless spectrum in the visible sector is just one of the MSSM.[5]

[5] In order to break $\mathcal{N} = 4$ SUSY in the unbroken gauge sector into $\mathcal{N} = 1$ SUSY, we would consider the toroidal orbifold background with trivial embedding. In such a case, the $SO(32)$ gauge group is broken down

Table 6. The VEV of dilaton $\langle S \rangle$ for the MSSM.

N	5	7	9
$\langle S \rangle$	2.93	1.83	1.33

Table 7. The values of B_2 and B_3 for the MSSM in the case of $N = 5, 7, 9$. By increasing the number of N appearing in the definition of $U(1)_Y$ (33), the values of B_i increase.

	Model 1 ($N = 5$)	Model 2 ($N = 7$)	Model 3 ($N = 9$)
B_2	−4.33	−0.88	0.69
B_3	−3.98	−0.53	1.04

In the case of MSSM, from the experimental values of the $U(1)_Y$ gauge coupling, $g^{-2}_{U(1)_Y}(M_s) = 2.44$ for the MSSM, the dilaton VEV $\langle S \rangle$ in Eq. (38) is determined by N as shown in Table 6 for $N = 5, 7, 9$. In what follows, we discuss the explicit models with $N = 5, 7, 9$.

Then, by solving Eq. (31) and the two-loop renormalization group equations for MSSM, we evaluate the ratio of gauge couplings at M_s as

$$\frac{\left\langle \mathrm{Re}\, f_{U(1)_Y} \right\rangle}{\left\langle \mathrm{Re}\, f_3 \right\rangle} = \frac{A\,(N)}{1 + \sum_k \beta_3^k \langle \mathcal{T}_k \rangle / \langle S \rangle} = \frac{g_3^2\,(M_s)}{g^2_{U(1)_Y}\,(M_s)} \simeq 1.468,$$
$$\frac{\left\langle \mathrm{Re}\, f_{U(1)_Y} \right\rangle}{\left\langle \mathrm{Re}\, f_2 \right\rangle} = \frac{A\,(N)}{1 + \sum_k \beta_2^k \langle \mathcal{T}_k \rangle / \langle S \rangle} = \frac{g_2^2\,(M_s)}{g^2_{U(1)_Y}\,(M_s)} \simeq 1.573, \tag{46}$$

where the experimental values such as the gauge coupling of $SU(3)$, $\alpha^{-1}_{SU(3)_C} \simeq 0.1184$, the Weinberg angle $\sin^2\theta \simeq 0.231$, and the fine-structure constant $\alpha \simeq 1/128$ at the electroweak scale are employed. From Eq. (46), we estimate the quantities in Eq. (41) in Table 7 for $N = 5, 7, 9$.

In the following, we employ the same magnetic flux configurations as in Sect. 4.1, denoted by models 1 ($N = 5$), 2 ($N = 7$), and 3 ($N = 9$), which are realistic in the sense that they include the gauge symmetry including $SU(3)_C \times SU(2)_L \times U(1)_Y$, three chiral generations of quarks and leptons without chiral exotics in the visible sector, and the experimental values of gauge couplings in Eq. (40); at the same time, they satisfy the consistency conditions in Sect. 2.3.

Within the range $2m_1^i \in [-15, 15]$, $1.0 \leq \langle \mathcal{T}_i \rangle \leq 3.5$, $i = 1, 2, 3$, and $1 \leq \mathrm{Vol}(M) \leq 10$, the magnetic flux configurations in models 1, 2, 3 with and without heterotic five-branes are determined as shown in Tables 3, 4, and 5, respectively. Although these flux configurations in all the models induce non-vanishing FI terms whose size is typically of $\mathcal{O}(M_s)$, we assume that such FI terms are canceled by the VEVs of certain scalar fields. In the case without five-branes in Tables 3, 4, and 5, Eq. (5) is satisfied by the $U(1)$ fluxes themselves, whereas, in the case with five-branes, the tadpole condition (5) is canceled by the existence of five-branes. Moreover, the magnetic fluxes in Tables 3, 4, and 5 predict the same values of gauge couplings at the string scale, because only m_1^i and m_2^i appear in the non-universal terms of the $SU(2)_L$ and $SU(3)_C$ gauge couplings.

by the existence of magnetic fluxes, whereas the adjoint matters are projected out by the orbifold projection. The details will be studied elsewhere.

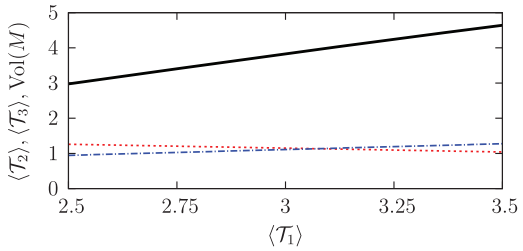

Fig. 6. The VEVs of moduli $\langle\mathcal{T}_2\rangle$ (red dashed curve), $\langle\mathcal{T}_3\rangle$ (blue dot-dashed curve), and the volume of three-tori $\mathrm{Vol}(M) = \langle\mathcal{T}_1\mathcal{T}_2\mathcal{T}_3\rangle$ (black thick curve) as a function of $\langle\mathcal{T}_1\rangle$ in model 1.

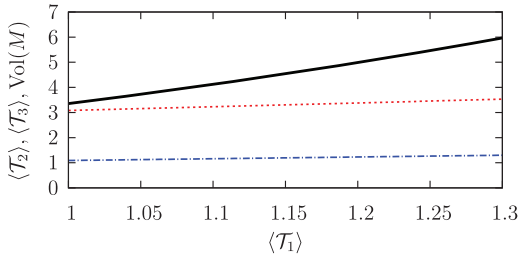

Fig. 7. The VEVs of moduli $\langle\mathcal{T}_2\rangle$ (red dashed curve), $\langle\mathcal{T}_3\rangle$ (blue dot-dashed curve), and the volume of three-tori $\mathrm{Vol}(M) = \langle\mathcal{T}_1\mathcal{T}_2\mathcal{T}_3\rangle$ (black thick curve) as a function of $\langle\mathcal{T}_1\rangle$ in model 2.

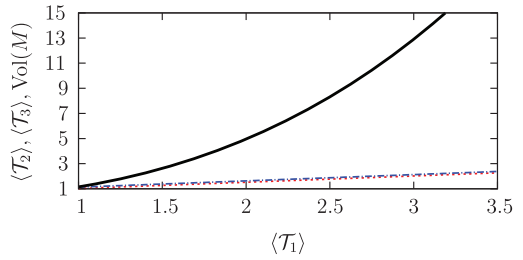

Fig. 8. The VEVs of moduli $\langle\mathcal{T}_2\rangle$ (red dashed curve), $\langle\mathcal{T}_3\rangle$ (blue dot-dashed curve), and the volume of three-tori $\mathrm{Vol}(M) = \langle\mathcal{T}_1\mathcal{T}_2\mathcal{T}_3\rangle$ (black thick curve) as a function of $\langle\mathcal{T}_1\rangle$ in model 3.

Finally, Figs. 6, 7, and 8 show the values of Kähler moduli and volume of three-tori $\mathrm{Vol}(M) = \langle\mathcal{T}_1\mathcal{T}_2\mathcal{T}_3\rangle$ as a function of $\langle\mathcal{T}_1\rangle$ in models 1, 2, and 3, respectively. The $\mathcal{O}(1)$ values of Kähler moduli in Figs. 6, 7, and 8 are consistent with the experimental values of gauge couplings in the MSSM. Similarly, we can analyze a wider region of $\mathcal{T}_{\min} < \langle\mathcal{T}_i\rangle < \mathcal{T}_{\max}$ with larger $\mathcal{T}_{\max}$ and smaller $\mathcal{T}_{\min}$.

5. Conclusion

We have studied $SO(32)$ heterotic models with $U(1)$ magnetic fluxes, which have gauge symmetry including $SU(3)_C \times SU(2)_L \times U(1)_Y$ and three chiral generations of quarks and leptons as well as vector-like matter fields. In contrast to $E_8 \times E_8$ heterotic string theory, there is non-universality among the gauge couplings of the standard model at the string scale and they depend on magnetic fluxes as well as the VEVs of the dilaton and Kähler moduli. Although there are several approaches to realizing gauge couplings consistent with the experimental values, they require large stringy threshold corrections by employing the large field values of Kähler moduli [3–5], which implies

large string coupling at the vacuum. In this paper, we have considered two SUSY breaking scenarios. One of them is that SUSY is broken at the string scale, whereas the other model is the TeV SUSY breaking scenario. In both scenarios, it was found that certain models can lead to gauge couplings consistent with the experimental values for $\mathcal{O}(1)$ of Kähler moduli values if moduli values as well as singlet VEVs are stabilized at proper values by a certain mechanism. Thus, we have constructed realistic models from both viewpoints of massless spectra and gauge couplings.

What is important for further study would be Yukawa couplings. The zero-mode profiles of quarks and leptons as well as Higgs fields are non-trivial because of the introduction of magnetic fluxes. That would lead to non-trivial Yukawa matrices.[6] Also, in Ref. [14], it was shown that the models with $N = 9$ have $SU(3)$ flavor symmetry. Such a flavor symmetry might be useful in realizing realistic values of fermion masses and mixing angles. We will study this issue elsewhere.

So far, we have taken the dilaton and Kähler moduli VEVs as free parameters in order to obtain gauge couplings consistent with the experimental values. Another future issue is to study moduli stabilization at proper values of the VEVs.

Acknowledgements

H. A. was supported in part by Grant-in-Aid for Scientific Research No. 25800158 from the Ministry of Education, Culture, Sports, Science and Technology (MEXT) in Japan. T. K. was supported in part by Grant-in-Aid for Scientific Research No. 25400252 and No. 26247042 from MEXT in Japan. H. O. was supported in part by Grant-in-Aid for JSPS Fellows No. 26-7296.

Funding

Open Access funding: SCOAP[3].

References

[1] P. H. Ginsparg, Phys. Lett. B **197**, 139 (1987).
[2] V. S. Kaplunovsky, Nucl. Phys. B **307**, 145 (1988); **382**, 436 (1992) [arXiv:hep-th/9205068] [Search INSPIRE] [erratum].
[3] L. J. Dixon, V. Kaplunovsky, and J. Louis, Nucl. Phys. B **355**, 649 (1991).
[4] I. Antoniadis, K. S. Narain, and T. R. Taylor, Phys. Lett. B **267**, 37 (1991).
[5] J. P. Derendinger, S. Ferrara, C. Kounnas, and F. Zwirner, Nucl. Phys. B **372**, 145 (1992).
[6] L. E. Ibanez, D. Lust, and G. G. Ross, Phys. Lett. B **272**, 251 (1991) [arXiv:hep-th/9109053] [Search INSPIRE].
[7] L. E. Ibanez and D. Lust, Nucl. Phys. B **382**, 305 (1992) [arXiv:hep-th/9202046] [Search INSPIRE].
[8] H. Kawabe, T. Kobayashi, and N. Ohtsubo, Nucl. Phys. B **434**, 210 (1995) [arXiv:hep-ph/9405420] [Search INSPIRE].
[9] T. Kobayashi, Int. J. Mod. Phys. A **10**, 1393 (1995) [arXiv:hep-ph/9406238] [Search INSPIRE].
[10] R. Altendorfer and T. Kobayashi, Int. J. Mod. Phys. A **11**, 903 (1996) [arXiv:hep-ph/9503388] [Search INSPIRE].
[11] D. Bailin and A. Love, J. High Energy Phys. **1504**, 002 (2015) [arXiv:1412.7327 [hep-th]] [Search INSPIRE].
[12] R. Blumenhagen, D. Lust, and S. Stieberger, J. High Energy Phys. **0307**, 036 (2003) [arXiv:hep-th/0305146] [Search INSPIRE].
[13] Y. Hamada, T. Kobayashi, and S. Uemura, Nucl. Phys. B **897**, 563 (2015) [arXiv:1409.2740 [hep-th]] [Search INSPIRE].
[14] H. Abe, T. Kobayashi, H. Otsuka, and Y. Takano, J. High Energy Phys. **1509**, 056 (2015) [arXiv:1503.06770 [hep-th]] [Search INSPIRE].

[6] For a relevant study on magnetized brane models, see, e.g., Refs. [32–35].

[15] K. S. Choi, T. Kobayashi, R. Maruyama, M. Murata, Y. Nakai, H. Ohki, and M. Sakai, Eur. Phys. J. C **67**, 273 (2010) [arXiv:0908.0395 [hep-ph]] [Search INSPIRE].
[16] T. Kobayashi, R. Maruyama, M. Murata, H. Ohki, and M. Sakai, J. High Energy Phys. **1005**, 050 (2010) [arXiv:1002.2828 [hep-ph]] [Search INSPIRE].
[17] R. Blumenhagen, G. Honecker, and T. Weigand, J. High Energy Phys. **0506**, 020 (2005) [arXiv:hep-th/0504232] [Search INSPIRE].
[18] R. Blumenhagen, G. Honecker, and T. Weigand, J. High Energy Phys. **0508**, 009 (2005) [arXiv:hep-th/0507041] [Search INSPIRE].
[19] J. Polchinski, *String Theory* (Cambridge University Press, Cambridge, UK, 1998), Vol. 2.
[20] T. Weigand, Fortsch. Phys. **54**, 963 (2006).
[21] E. Witten, Nucl. Phys. B **460**, 541 (1996) [arXiv:hep-th/9511030] [Search INSPIRE].
[22] M. J. Duff, R. Minasian, and E. Witten, Nucl. Phys. B **465**, 413 (1996) [arXiv:hep-th/9601036] [Search INSPIRE].
[23] G. Aldazabal, A. Font, L. E. Ibanez, A. M. Uranga, and G. Violero, Nucl. Phys. B **519**, 239 (1998) [arXiv:hep-th/9706158] [Search INSPIRE].
[24] M. B. Green, J. H. Schwarz, and P. C. West, Nucl. Phys. B **254**, 327 (1985).
[25] L. E. Ibanez and H. P. Nilles, Phys. Lett. B **169**, 354 (1986).
[26] R. Blumenhagen, S. Moster, and T. Weigand, Nucl. Phys. B **751**, 186 (2006) [arXiv:hep-th/0603015] [Search INSPIRE].
[27] E. Witten, Phys. Lett. B **149**, 351 (1984).
[28] E. Witten, J. High Energy Phys. **9812**, 019 (1998) [arXiv:hep-th/9810188] [Search INSPIRE].
[29] A. M. Uranga, Nucl. Phys. B **598**, 225 (2001) [arXiv:hep-th/0011048] [Search INSPIRE].
[30] K. A. Olive et al. [Particle Data Group Collaboration], Chin. Phys. C **38**, 090001 (2014).
[31] L. E. Ibanez, F. Marchesano, and R. Rabadan, J. High Energy Phys. **0111**, 002 (2001) [arXiv:hep-th/0105155] [Search INSPIRE].
[32] D. Cremades, L. E. Ibanez, and F. Marchesano, J. High Energy Phys. **0405**, 079 (2004) [arXiv:hep-th/0404229] [Search INSPIRE].
[33] H. Abe, K. S. Choi, T. Kobayashi, and H. Ohki, Nucl. Phys. B **814**, 265 (2009) [arXiv:0812.3534 [hep-th]] [Search INSPIRE].
[34] H. Abe, T. Kobayashi, H. Ohki, A. Oikawa, and K. Sumita, Nucl. Phys. B **870**, 30 (2013) [arXiv:1211.4317 [hep-ph]] [Search INSPIRE].
[35] H. Abe, T. Kobayashi, K. Sumita, and Y. Tatsuta, Phys. Rev. D **90**, 105006 (2014) [arXiv:1405.5012 [hep-ph]] [Search INSPIRE].